Journal of the European Ceramic Society 20 (2000) 1205–1213

Influence of annealing on the mechanical properties of SiC–Si composites with sub-micron SiC microstructures

Matthias Wilhelm*, Werner Wruss

Institute for Chemical Technology of Inorganic Materials, University of Technology of Vienna, Austria

Received 22 April 1999; received in revised form 17 September 1999; accepted 6 October 1999

Abstract

The influence of annealing temperature (1000, 1100 and 1200°C) on the mechanical properties of SiC–Si composites has been evaluated. Three SiC powders with particle sizes in the range of 0.24 to 0.7 μm were used to produce the composites. Before application the SiC powders were treated with hydrofluoric acid to remove the extent of SiO_2. With this treatment a successful infiltration of green-bodies especially produced of SiC powder with a mean particle size of 0.24 μm was possible. The bending strength decreased with decreasing SiC starting particle size as well as with increasing annealing temperature. However, the fracture toughness was independent on SiC starting particle size and annealing temperature. XRD diffraction analysis showed that internal stress, expressed by broadening of XRD peaks, is low and had no effects on the mechanical properties of the composites.

Keywords: Annealing; Composites; Mechanical properties; Microstructure-final; SiC–Si

1. Introduction

Silicon-infiltrated silicon-carbide (SiSiC, SiC–Si, RB-SiC) is a well known material for high performance ceramics such as heat-exchangers, seal-rings, valve-discs and ceramic engine parts.[1–3] This ceramic has particular advantages in terms of producing and costs since such ceramic parts can be produced at relatively low temperatures (1500–1700°C) with no or less shrinkage so net-shape processing is possible. The great field of applications are due to its outstanding properties like good resistance against oxidation and corrosion, excellent tribological properties and high mechanical strength up to 1300°C.[4–7] The basic mode of manufacturing SiC–Si ceramics consists of infiltrating a porous compact of α-silicon carbide (SiC) and carbon with liquid silicon (Si). The carbon reacts with liquid silicon under formation of new β-SiC which grows onto the original α-SiC and hence bonds the whole compact together.[8] Residual pores and space not occupied by silicon carbide are filled with liquid silicon (free silicon phase). It is well known [9] that one limiting factor to obtain such ceramics is the amount of free silicon in the composites. At temperatures above 1400°C the mechanical properties (e.g. strength and creep) deteriorate due to existing free silicon content. The mechanical strength of SiC–Si is dependent on the grain size of the original SiC powder as well as on the amount of free silicon. With decreasing grain size of the original SiC powder and at comparable free silicon contents strength increases. Experiments of the authors have shown that using SiC powders with a mean grain size in the range of 3 to 12.8 μm a clear linear enhancement of the bending strength with decrease of original SiC size was observed.[10] However, a further reduction of the SiC particle-size (0.5 μm) brought no increase of the bending strength. One possible explanation of this behaviour was the occurrence of internal stress in the compacts as a result of the volume expansion of silicon during cooling. Due to the fine SiC microstructure, the silicon cannot expand during solidification as it should and this circumstance may be generate stresses within the microstructure. It was assumed that these internal stresses weaken the microstructure of the compacts produced and lower the bending strength of the material.[10]

* Corresponding author. Tel.: +43-1-58801-16130; fax: +43-1-587-79-18.

E-mail address: mwilhelm@fbch.tuwien.ac.at, http://aotech1.tuwien.ac.at/institut/oxidchemie/index.htm (M. Wilhelm).

0955-2219/00/$ - see front matter
PII: S0955-2219(99)00275-7

The present work in continuation of these works deals with the production of SiC–Si composites with submicron SiC grain structure. The grain size of the starting SiC is in the range of 0.24 to 0.7 μm. The assumed residual stresses of the composites shall be reduced by annealing at different temperatures and determined by X-ray diffraction analysis. To eliminate the influence of SiO_2 on the infiltration of the green-compacts the SiC powders used in this study shall be etched.

2. Experimental procedure

α-SiC powders (0.7, 0.51, 0.24 μm), carbon black, phenolformaldehyd resin (Perstorp AG, Sweden) and Si-metal (Gesellschaft für Elektrometallurgie, Germany, mean Si-grain size 0.2 μm) were used as starting materials. The SiC powders were provided by two suppliers, ESK Kempten Germany (0.7 μm SiC) and H.C. Starck, Waldshut-Tiengen, Germany (0.54 and 0.24 μm). Table 1 shows the typical characteristics of the SiC powders used and Table 2 gives the chemical composition of the silicon.

The analysis of the particle-size of the SiC powders used was carried out semi-automatically with the computer program Kontron KS100 by Zeiss: based on SEM images the SiC particles (about 130 for each SiC powder) were surrounded with a digitiser pen to get digitised values for the particle-perimeter (Fig. 1). From these values the mean particle-sizes of the SiC powders were then calculated.

To reduce the extend of SiO_2 of the SiC powders used in this study, the SiC powders were etched 24 h with 20 vol% hydrofluoric acid.

Table 1
Characteristics of the SiC-powders used

SiC-quality	Mean SiC-particle size (μm)	Oxygen content (wt%)	
		As supplied	After etching
RS 07	0.7	0.6	0.03
UF-15	0.51	1.7	0.6
UF-45	0.24	4.5	1.5

Table 2
Chemical composition of the silicon used

Mean SiC-particle size (μm)	Purity (w%)
0.2	Si: > 99.7; Fe: 0.004; B: 0.003; Co: 0.008; Cr: 0.01; Cu: 0.015; Mo: 0.002; Ni: 0.02; Nb: 0.002; Ta: 0.002; V: 0.03; W: 0.003; Ti: 0.05; Sn: 0.003; Zn: 0.003

Previous experiments by the authors have shown that it was impossible to produce SiC–Si composites with no open porosity using 0.24 μm SiC (density less 90%).[10] After infiltration, composites with high porosity (12%) were obtained and in some cases the green-compacts were destroyed during infiltration process. This behaviour was explained by the reactions of liquid silicon and free carbon, respectively, and the SiO_2 layer which covers as an oxidation product every SiC particle. It is quite clear, the smaller the grain size of SiC powders the higher the amount of SiO_2. The reaction between molten silicon and free carbon, respectively, and SiO_2 form gaseous products, CO and SiO, which leave the green-compacts during infiltration and hinder in that way the liquid silicon to flow into the green-compacts. However, a low content of oxygen (a thin layer of SiO_2) is necessary for a complete infiltration.[11] The produced SiO itself reacts with the near-surface carbon and opens in that way near-surface pores.

One possible way to obtain dense SiC–Si composites with a submicron SiC microstructure is to remove most of SiO_2 by etching with aqueous HF. As Table 1 shows, the extent of silica expressed by the oxygen content of the SiC powders as well as the excess of agglomeration can be clearly reduced by etching (Fig. 2). However, the reduction of SiO_2 by etching of 0.51 and 0.24 μm SiC powders was not so effective as expected (only a reduction to one third). This result can be explained by a re-oxidation during processing of the SiC powders.

To produce a porous green-compact the etched α-SiC-powder (85 wt%) and the soot (5 wt%) were suspended in acetone and were homogenised for 24 h in a tumbling mixer. The phenolformaldehyd resin (10 wt%, organic binder) was then added and the acetone was removed to obtain a dry product. The dried powder-mixture was sieved, granulated by rolling the moist powder in a flask and then dry pressed at 75 MPa to get green-compacts measuring approximately $50\times40\times4$ mm^3.

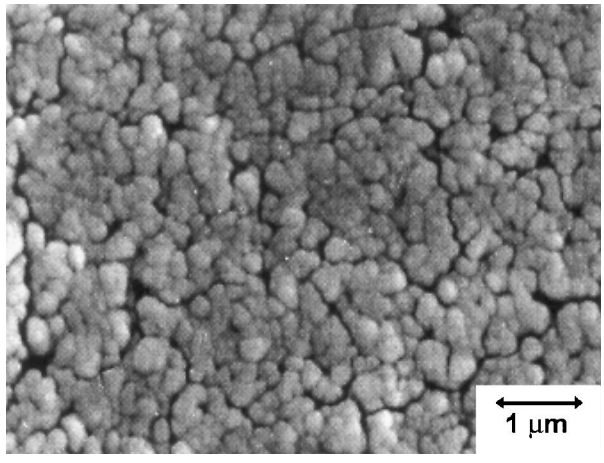

Fig. 1. SEM-image of UF-45-SiC powder with a mean particle-size of 0.24 μm as supplied.

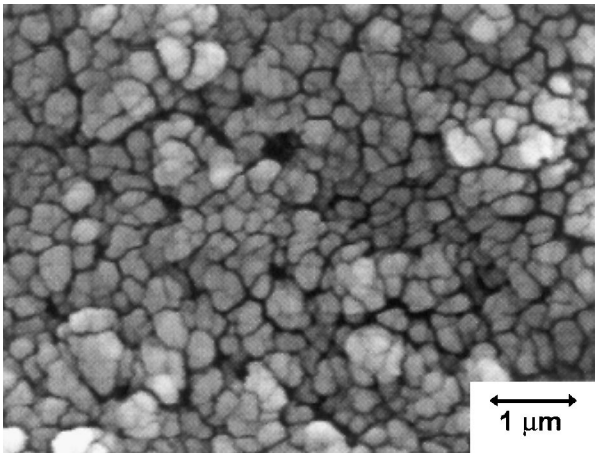

Fig. 2. SEM-image of UF45-SiC powder with a mean particle-size of 0.24 μm after etching with HF.

After pressing, the green-compacts were heated up under controlled conditions to harden and crack the organic binder to pure carbon. The contact-infiltration technique was used to silicide the green-bodies. In this technique a silicon source (consisting of high purity silicon and carbon) is placed on the top of the green body, placed in a graphite furnace and heated under vacuum (typically 5×10^{-5} bar) at 1500°C for 60 min.

After infiltration the excess of silicon remained on the surface was removed by grinding and the compacts were then annealed 50 h at 1000, 1100 and 1200°C in Argon atmosphere in a tube furnace and a heat rate of 5°C/min. The subsequent cutting of the material was performed with a diamond saw (bars measuring $40\times3\times4$ mm^3). The bars were polished with diamond grit of a range of sizes down to 1 μm. The bulk density of the infiltrated specimens was measured by Archimedes principle in water.

The fracture toughness of the composites was measured using three-point loading and single-edge notched beam technique with a notch width of 100 μm, a span of 11 mm and a cross head speed of 0.5 mm/min (nine specimens for every material) at room temperature. The broken bars of the fracture toughness measurements were used to determine bending strength. Bending strength was measured on $20\times3\times4$ mm^3; bars (18 bars for every material is sufficient for determining bending strength) at room temperature using three point loading with a span of 11 mm and a cross-head speed of 0.2 mm/min and were evaluated using Weibull statistics.

3. Results and discussion

3.1. Density

The Table 3 shows the measured densities of the green-compacts. Fig. 3 represents the dependence of the

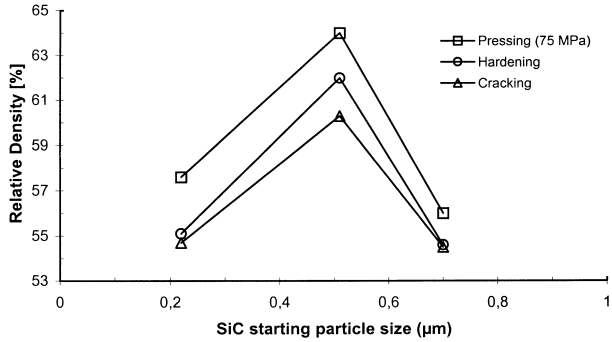

Fig. 3. Relative densities as a function of particle-size of SiC-powder on SiC–Si (data point sizes represent the standard deviation).

green-compact-densities (% of theoretical density) after compaction, hardening and cracking on the particle-size of the used SiC. The calculation of theoretical densities is described in Ref. 12. The volume fraction of free silicon within the composites can be estimated by the equation using theoretical densities of SiC (3.21 g/cm^3) and Si (2.33 g/cm^3) e.g. $V_{Si}=3.648-1.136D$, where D is the bulk density of the composites.

Table 2 shows the density-values after compaction, hardening, cracking and infiltration compared to the theoretical density.

After infiltration fully dense composites made of 0.7 μm SiC and 0.51 μm SiC powder were obtained. Due to the treatment with HF-acid a successful infiltration with liquid silicon of green-compacts with a 0.24 μm α-SiC structure could be carried out although the oxygen content was still high. This shows that for a successful infiltration a certain amount of oxygen is necessary. A porosity of 2% was observed at materials made of 0.24 μm SiC powder.

In general, the highest green-compact-densities were obtained using SiC powder with a mean particle size of 0.51 μm. It is interesting to note that the use of 0.24 μm SiC caused higher densities compared to compacts made of 0.7 μm SiC. It is assumed that due to the treatment with HF-acid the behaviour of the SiC powders (especially 0.51 and 0.24 μm SiC powders) in terms of compaction has changed. The etching with HF-acid destroyed most of the agglomerates. In previous experiments these agglomerates had hindered the compaction of the green-compacts using untreated SiC powders.

3.2. Microstructural analysis

Scanning electron micrographs as well as BSE analysis of the polished surfaces of the composites show isotropic microstructures and homogeneously distributed free silicon phase. All the composites were found to be fully dense except composites made of 0.24 μm SiC starting powder were some pores were observed.

Optical analysis of the polished surfaces (not shown) showed that all composites have homogeneous dispersed

free silicon phase with low frequency of pressing failures like big silicon islands or different dense areas within the microstructure. It has to be noted that no influence of annealing temperature could be determined on the microstructures (e.g. grain growth of starting SiC) of the composites.

During infiltration procedure no effective grain growth of the starting SiC particles took place. The starting SiC grains observed are combined together with new formed SiC and are embedded into free silicon phase (Fig. 4).

Examination of all fractured surfaces of the composites with SEM showed that most of the fractures originated from defects near the surfaces. These defects were found to be pores as well as silicon islands which are surrounded by a layer of SiC, respectively, within the microstructure. Fig. 6 illustrates such an defect. The bright dots in Fig. 5 were investigated by EDS analysis and were found to be not heavy metal silicides. It seems that these areas are charged by the electron beam. The differences between BSE and SEI images are low and reveal only less information about the microstructure. This may due to the high amount of free silicon phase and the very fine SiC microstructure of the composites.

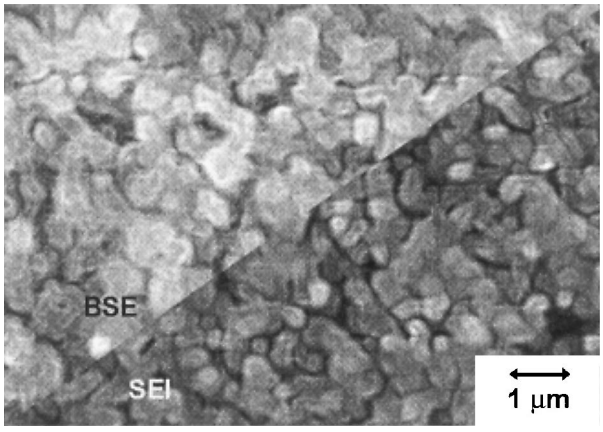

Fig. 4. SEI/BSE split image of polished surface of SiC–Si illustrating the structure made of 0.24 μm (annealed at 1000°C, unetched).

It is interesting to note that within the free silicon microcracks were found. These microcracks can be observed in all annealed composites at all annealing temperatures and were observed only in the middle of the fractured surfaces but were not found in unannealed composites or in silicon islands located near the surfaces. Because such microcracks were not found in unannealed composites it is assumed that these microcracks are generated due to local tensile stresses generated during cooling down in the annealing procedure due to crystallographic mismatch and/or differences in thermal expansion coefficient of SiC and silicon. However, X-ray diffraction analysis has shown that the effect of tensile stresses on the peak broadening of the silicon peaks is very low and can be neglected.

The fractured surfaces of composites produced of 0.24 μm SiC starting powder revealed that often the fractures originated from processing defects e.g. pores which are not filled with silicon (Fig. 7). Figs. 8 and 9 illustrate that SiC particles found within the pore are partially covered by silicon. Up to now it is not fully understood why the pore is not filled up with silicon. However, at the side of the pore free silicon was observed. It may be assumed that a certain gas pressure (CO or SiO gas) within the pore had hindered the liquid silicon to fill up the pore.

3.3. XRD-analysis

The X-ray diffraction analysis was carried out in terms of determining internal stresses. Stresses within

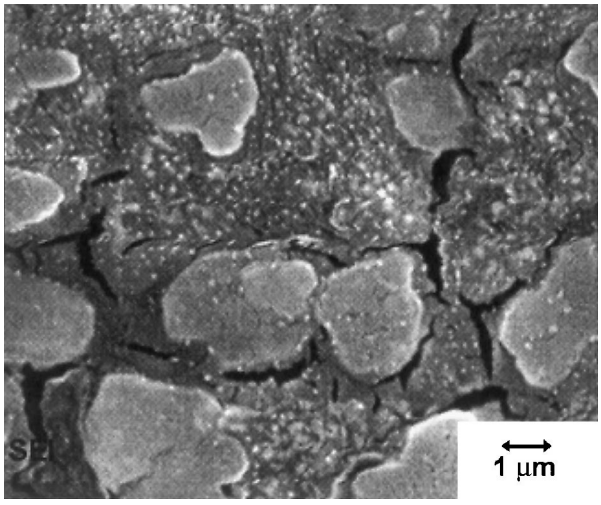

Fig. 5. SEM micrograph of the fractured surface of the composite made of 0.51 μm SiC (annealed at 1000°C) illustrating microcracks within silicon phase.

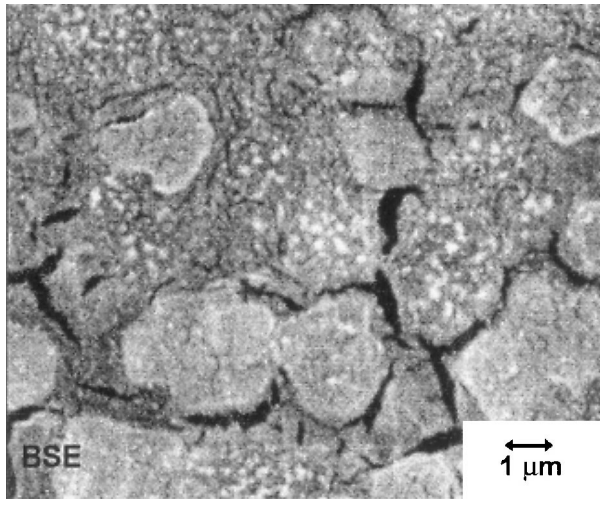

Fig. 6. BSE micrograph of the fractured surface of the composite made of 0.51 μm SiC (annealed at 1000°C) illustrating microcracks within silicon phase.

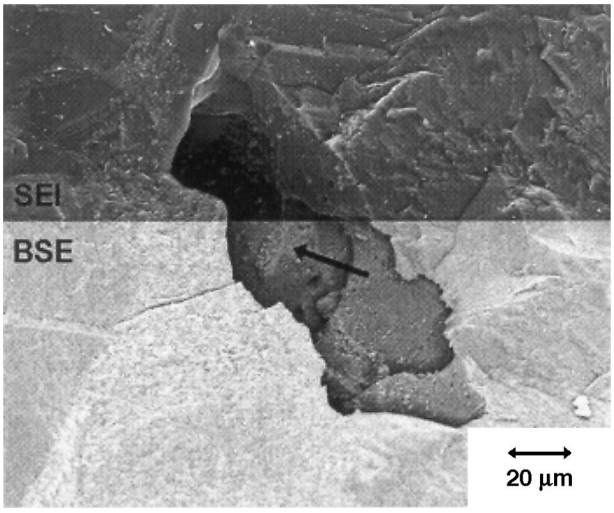

Fig. 7. SEI/BSE split image: pore within the fractured surface of the composite made of 0.24 µm SiC (unannealed); arrow indicates detail region of Figs. 8 and 9.

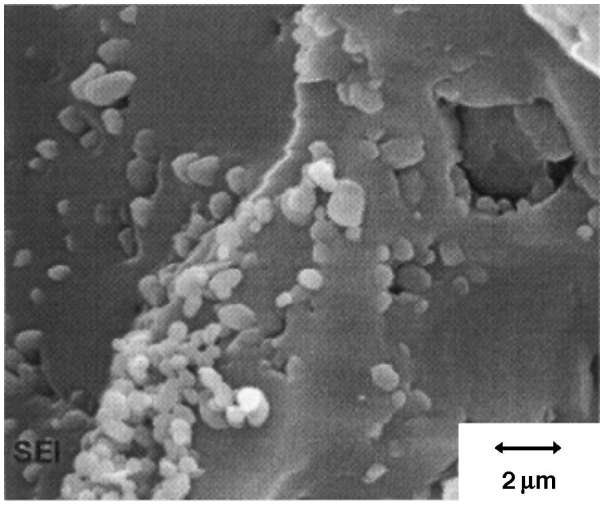

Fig. 8. SEM image: detail of Fig. 7; look within the pore. SiC grains are embedded within silicon.

the microstructure may be possibly generated because during cooling the free silicon phase expands. In this investigation the volume fraction of free silicon increased with decreasing SiC starting particle size. It was assumed that internal stresses is lowering the mechanical properties of the composites and is proportional to the volume fraction of free silicon.

One possibility to determine stress of the composites is the measuring of the X-ray diffraction peak-broadening. This method was used to determine the lattice distortion of alumina powder generated through milling.[13] However, the effects are quite small, which means that accurate measurements are necessary. The peak-broadening is influenced by a number of factors, e.g. instrumentation broadening, crystallite-size and microstrains expressed by lattice distortion. In this investigation only composites produced of 0.24 µm SiC starting powder

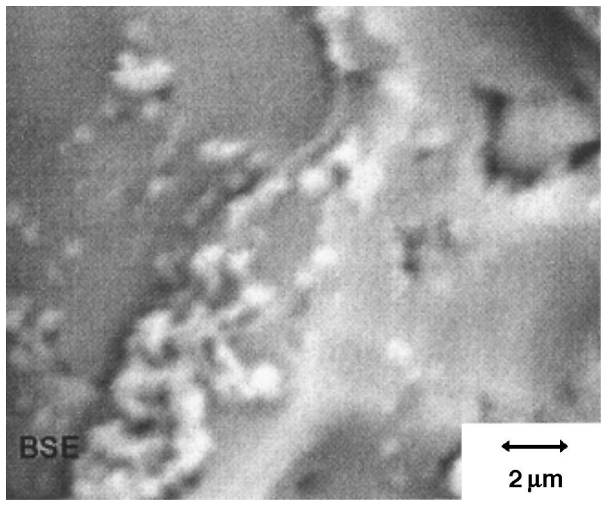

Fig. 9. BSE image: look within the pore. SiC grains are embedded within silicon.

have been measured due to the consideration that these composites have the biggest influence on the peak-broadening due to their enhanced free silicon content. The measurements were carried out using Philips PW 1710 equipped with graphite monochromator and operated at 40 kV and 40 mA using CuK_α radiation in step scan mode with 0.02°/step and 1.2°/min in the range of 5 to 130°.

The analysis of the XRD-plots by Rietfeld method[14] has shown that the effect of residual stresses on the peak-broadening can be neglected. No evidence of residual stresses was observed. The small peak-broadening observed at unannealed composite was due to the small grain size of free silicon phase. Because of the clear grain growth of silicon during annealing the XRD peaks of silicon became smaller. It was found that the crystallite size of silicon after annealing at 1200°C was 2 times higher than the crystallite size of silicon after annealing at 1000°C. XRD pattern of the composite produced of 0.24 µm starting SiC powder and annealed at 1000°C indicates the presence of free silicon, α-SiC, small amounts of β-SiC and 4H-SiC (main peak at position 34.8° 2θ). During the reaction between free carbon and molten silicon β-SiC is formed which subsequently is transformed to an array of polytypes controlled by the structure of the starting material.[15–18] However, in most of these studies reported starting SiC powders with grain sizes in the range of 5 to 100 µm were used. It must be emphasised that in this study sub-micron SiC powders were used. The differences between α-SiC (starting material) and 4H-SiC (new material) is the different length of the *c*-axis of the elementary cell (α-SiC: 15 Å, 4H-SiC: 10 Å) but both, α- and 4H-SiC, have got hexagonal modification. After infiltration it was found that most of new formed SiC had been transformed to 4H-SiC. Only a few percent (approximately 3 wt%) of β-SiC (cubic modification) are deposited on the

starting SiC particles. This result was found possibly either due to boron impurities (BN_{hex} is used as a coating to prevent reaction with graphite crucible) and/or the very fine grain size of the starting SiC particles (hexagonal modification) which force the transformation into a hexagonal structure of the new formed SiC. Experiments have shown that in microstructures made of coarse starting SiC particles (13 μm) after infiltration predominantly β-SiC was found. Also, it is interesting to note that after infiltration (at same infiltration conditions) the residue of the silicon source consisted of approximately 50 wt% of β-SiC, silicon and very small amounts of 4H-SiC (< 2 wt%). These results show that not only impurities or (local) temperatures control the SiC transformation, the transformation maybe also influenced (''seeded'') by the fine SiC microstructure.

3.4. Mechanical properties

To calculate the critical defect sizes the classical fracture mechanical relationship is applied which corresponds to Griffith criterion:

$$\sigma \cdot Y \cdot \sqrt{\pi \cdot a} \equiv K \geqslant K_{Ic} \tag{1}$$

where σ is the load amplitude, a the crack length, Y a geometric factor, K the stress intensity factor and K_{Ic} the fracture toughness. Using this equation the critical defect radius is

$$a_c = \frac{1}{\pi} * \left(\frac{K_{Ic}}{Y\sigma_B}\right)^2 \tag{2}$$

with σ_B as the fracture strength and $Y = 2/\pi$ for a penny-shaped short crack. The independently measured values for fracture strength and fracture toughness were set in Eq. (2) to calculate the critical defect sizes.

The dependence of the critical defect size on the SiC starting particle size and annealing temperature is illustrated in Fig. 11.

The critical defect size is more or less the same for all unannealed materials. This result shows that the critical defect size is independent on the SiC starting particle size as well as the content of free silicon. With decreasing starting SiC particle size and increasing annealing temperature the critical defect sizes observed increased for the composites. It is interesting to note that at 1000°C annealing temperature the critical defect sizes reached their lowest values for all materials. The microstructural analysis of the fracture origins confirmed the calculated defect-diameters.

The mechanical properties of the composites are summarised in Tables 4 and 5. The fracture toughness and mean bending strength are plotted as a function of the particle-size of starting α-SiC and annealing temperature and are demonstrated in Figs. 12 and 13.

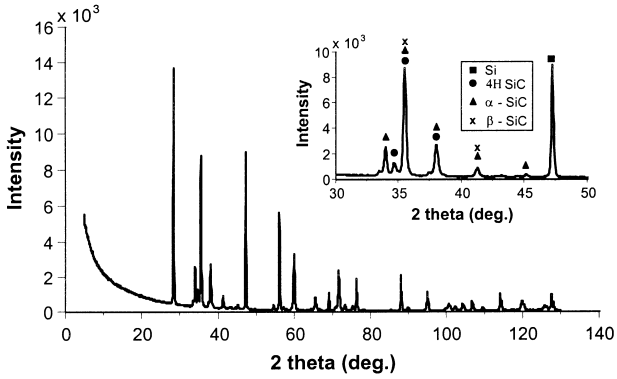

Fig. 10. XRD pattern of SiC–Si composite of 0.24 μm SiC (annealed at 1000°C).

In general, the fracture toughness is independent on the SiC starting particle size as well as on the annealing temperature and has a value of 3.8 ±0.6 MPa $\sqrt{m}$. However, a slight increase of fracture toughness with decreasing SiC starting particle size is observed for the unannealed materials. The mean bending strength values decreased with decreasing SiC starting particle size. In general, the lowest strength values were obtained for the composites made of 0.24 μm SiC powder whereas the highest bending strength value (516 MPa) was observed for the composite made of 0.51 μm SiC powder and annealed at 1000°C.

With increasing annealing temperature up to 1000°C the bending strength first remained constant for all composites but then clearly decreases. The lowest bending strength values were observed at 1200°C annealing temperature for all composites due to the enhanced critical defect size of the composites (Table 5). Due to poor mixing in the compact often areas of SiC free residual silicon (radius 30–40 μm) surrounded or almost closed by a layer of fine SiC were found in the composites. The enhancement of the critical defect size can be explained by the fact that a certain grain growth of the free silicon occurred during annealing of the materials and it is understandable that with increasing annealing temperature the grain growth of free silicon increases, too. This circumstance leads to big silicon grains which may act as fracture initiating defects during testing bending strength. It is known that the weak parts in the Si–SiC microstructure are the SiC:Si interfaces[18] as well as the free silicon itself. Due to the very fine microstructure of the composites more SiC:Si interfaces are within the structure compared to those made of coarse SiC. The crystallographic matching between Si and SiC (untransformed as well as transformed) is poor. It is assumed that with increasing annealing temperature the crystallographic matching becomes additionally poorer and lowers in that way the strength.

Although the initial purity of the silicon used to produces the composites is very high (Table 2) it can not be excluded that the formation of impurity silicides, e.g.

Table 3
Density values obtained after compaction, hardening, cracking and infiltration for each SiC powder

SiC-quality/mean particle size (μm)	Density after compaction (g/cm^3)	Density after hardening (g/cm^3)	Density after cracking (g/cm^3)	Density after infiltration (g/cm^3)	Free silicon content (Vol%)	Theoretical density (g/cm^3)
RS 07/0.7	1.60 ± 0.01 (56.0%)	1.56 ± 0.01 (54.6%)	1.56 ± 0.014 (54.6%)	2.86 ± 0.001 (100%)	39 ± 1	2.86 ± 0.004 (100%)
UF-15/0.51	1.85 ± 0.03 (64.0%)	1.79 ± 0.03 (62.0%)	1.75 ± 0.01 (60.3%)	2.89 ± 0.001 (100%)	35 ± 0.8	2.89 ± 0.003 (100%)
UF-45/0.24	1.60 ± 0.01 (56.0%)	1.57 ± 0.01 (55.1%)	1.56 ± 0.02 (54.7%)	2.79 ± 0.002 (98.0%)	42 ± 1	2.85 ± 0.007 (100%)

Table 4
Description of the mechanical properties of the SiC–Si composites

SiC-quality/particle-size (μm)	Fracture toughness (MPa$\sqrt{m}$)				Mean bending strength σ_{B50} (MPa)			
	Annealing temperature				Annealing temperature			
	Unannealed	1000°C	1100°C	1200°C	Unannealed	1000°C	1100°C	1200°C
RS07/0.7	4.4 ± 0.4	3.4 ± 0.7	3.8 ± 0.6	3.4 ± 0.7	499 ± 35	494 ± 40	407 ± 42	414 ± 49
UF-15/0.51	4.8 ± 0.6	4.4 ± 0.5	3.3 ± 0.4	4.6 ± 0.5	512 ± 48	516 ± 42	388 ± 55	436 ± 48
UF-45/0.24	3.4 ± 0.6	3.0 ± 0.5	3.2 ± 0.4	3.6 ± 0.6	387 ± 33	411 ± 37	378 ± 32	336 ± 30

Table 5
Critical defect sizes and Weibull moduli of the SiC–Si composites

SiC-quality/particle-size (μm)	Critical defect size (μm)				Weibull modulus			
	Annealing temperatures				Annealing temperatures			
	Unannealed	1000°C	1100°C	1200°C	Unannealed	1000°C	1100°C	1200°C
RS07/0.7	61 ± 3	37 ± 8	68 ± 8	53 ± 10	6 ± 2	4 ± 2	3 ± 2	4 ± 2
UF-15/0.51	69 ± 5	57 ± 4	57 ± 3	87 ± 1	4 ± 2	5 ± 2	4 ± 1	4 ± 1
UF-45/0.24	61 ± 10	42 ± 6	56 ± 5	90 ± 10	5 ± 2	4 ± 2	5 ± 2	4 ± 2

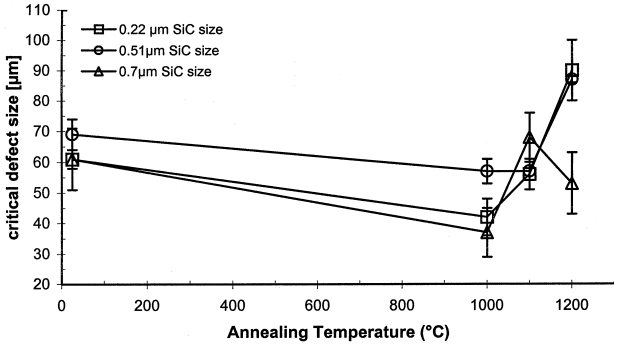

Fig. 11. Critical defect size versus annealing temperature in SiC–Si composites.

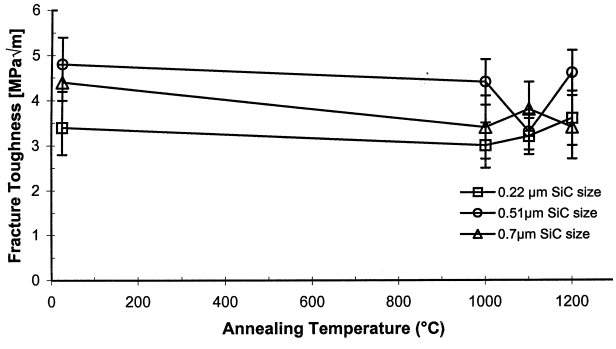

Fig. 12. Fracture toughness versus particle-size of α-SiC-powder in SiC–Si composites.

chrome, iron, deteriorate also the strength. However, these silicides must be present in all composites and their presence must be independent of the annealing temperature. EDS analysis of all fractured surfaces showed no evidence of the occurrence of such heavy metal silicides.

Microstructural analysis of the fractured surfaces revealed that most of the fractures originated from silicon islands and pores near the surface. These defects can be eliminated by improved mixing technique, e.g. attrition milling. The fact that at 1000°C annealing temperature the bending strength remained at a high level can explained by healing of microcracks within the free silicon phase which were induced during cooling step or by polishing. In Ref. 18 the authors have shown that during polishing the Si from the SiC:Si interfaces

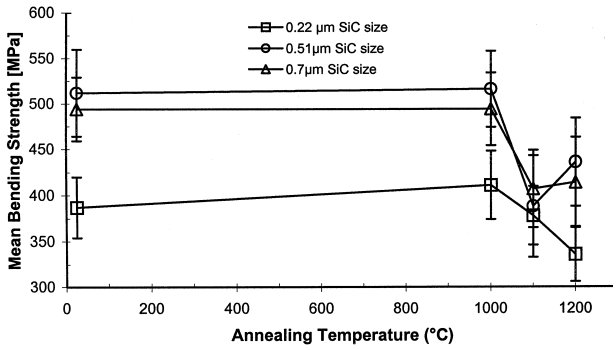

Fig. 13. Variation of mean bending strength with annealing temperature in SiC–Si composites.

was broken out of the surface and hence these places act as initial flaws for fracture. Such failures can not be excluded for the samples investigated because the time for cutting, grinding and polishing was clearly enhanced compared to the composites produced of coarse starting SiC[10] and may contribute to the decrease of strength. Fig. 6 illustrates microcracks within a silicon island. The healing of microcracks and the grain growth of silicon are two contrary effects. At lower annealing temperatures the healing of microcracks predominate the small grain growth of silicon and high strength values were obtained. Internal stresses, in principal, could also influence the mechanical behaviour. However, the residual stresses observed by XRD-analysis was low. With increasing of annealing temperature the situation changes. The grain coarsening of free silicon predominate the healing of microcracks and hence the bending strength values decrease. The Weibull modulus as an expression of the homogeneity is low which shows the imperfect powder processing.

4. Conclusions

In this investigation, three commercial SiC powders with grain sizes in the range of 0.24 to 0.7 µm were used to produce SiC–Si composites with submicron SiC microstructure. The influence of annealing on the mechanical properties as well as microstructure was investigated:

1. Due to the treatment of the starting SiC powders with hydrofluoric acid in terms of removing the extent of SiO_2 a successful infiltration of the green-compacts especially of green-compacts produced of 0.24 µm starting SiC powder can be obtained.
2. The produced composites were annealed at 1000, 1100 and 1200°C in terms of reducing the assumed stresses within the microstructure. The bending strength increased in the range of room temperature to 1000°C. A drastically decrease of strength was observed after annealing at 1100 and 1200°C, respectively. The decrease of strength is caused by the growth of critical defects during annealing, microcracks induced by tensile stress generated during cooling down in the annealing step and the presence of low amounts of heavy metal silicides. The highest bending strength value (516 MPa) was obtained at 1000°C annealing temperature for the composite consisted of 0.51 µm starting SiC. The fracture toughness was independent of the SiC particle size as well as annealing temperature.
3. The effects of internal stresses on the mechanical properties were found very low and were independent of annealing temperatures. However, microcracks within the microstructure may be indicative for (tensile) stresses generated during cooling down the samples in the annealing step because such microcracks were only found in annealed composites.
4. The critical defects were found to be silicon islands and pores. Within these silicon islands often microcracks were observed. XRD analysis showed that the silicon grows during annealing. It is well known that with lowering the starting grain size of SiC the processing (mixing, compaction) of the composites becomes more difficult.
5. After infiltration small amounts of β-SiC and more 4H-SiC was found for the composites. It seems that the small SiC microstructure force the transformation of β to 4HSiC.

Acknowledgements

We greatly acknowledge the support of this work by the Jubiläumsfonds der Österreichischen Nationalbank, Project No. P6281. The authors would like to thank University Professor Dr. R. Danzer (Univeristy of Leoben) for helpful discussions, and University Professor Dr. F. Kubel, Institute for Mineralogy, Cristallography and Structural Chemistry (TU-Vienna), for doing the XRD investigations.

References

1. Popper, P., The preparation of dense self-bonded silicon carbide. In *Special Ceramics*. Heywood, 1969, pp. 209–219.
2. Sawer, G. R. and Page, T. F., Microstructure characterisation of REFEL (reaction-bonded) silicon carbides. *J. Mat. Sci*, 1978, **13**, 885–904.
3. Trantina, G., Design techniques for ceramics in fusion reactors. *Nucl. Eng. Des*, 1979, **54**(1), 676–677.
4. Willerment, P. A., Pettand, R. A. and Whalen, J. J., Development and processing of injection-moldable reaction-sintered SiC compositions. *Am. Ceram. Soc*, 1978, **57**(8), 744–747.

5. John, B. and Wachtman, J., *Structural Ceramics*. Vol. 29, Academic Press, 1989, pp. 91–163.
6. Lim, C. and Iseki, T., Transport of fine-grained β-SiC/liquid Si system. *Adv. Ceram. Mater*, 1989, **3**, 291–293.
7. Krauth, A. et al., Ingenieurkeramische Bauteile für Anwendungen in der Energietechnik, Verfahrenstechnik, Metallurgie und Motorenbrau, Keramische Komponenten für Fahrzeug-Gasturbinen III. Springer Verlag, 1984, pp. 647.
8. Ness, N. J. and Page, T. F., Microstructural evolution in reaction bonded silicon carbide. *J. Mater. Sci.*, 1986, **21**, 1377–1397.
9. Chakrabati, O., Ghosh, S. and Mukerji, J., Influence of grain size, free silicon content and temperature on the strength and toughness of reaction-bonded silicon carbide. *Ceramics International*, 1994, **20**, 283–286.
10. Wilhelm, M., Kornfeld, M. and Wruss, W., Development of SiC — Si composites with fine-grained SiC microstructures. *J. Eur. Ceram. Soc.*, 1999, **19**, 2155–2163.
11. Forrest, C.W., Kennedy, P. and Shennan, J.V., The fabrication and properties of self-bonded silicon carbide bodies. TRG Report 2053 (S), 1970.
12. Forrest, C., Kennedy, P. and Shennan, J., The fabrication and properties of self-bonded silicon carbide. In *Special Ceramics*, Vol. 5. Heywood, 1972, pp. 99–123.
13. Ekström, T., Chatfield, C., Wruss, W. and Maly-Schreiber, M., The use of X-ray diffraction peak-broadening analysis to characterize ground Al_2O_3 powders. *J. Mater. Sci*, 1985, **20**, 1255–1274.
14. Taylor, J. C., Conputerprograms for standardless quantitative analysis of minerals using the full power diffraction profile. *Powder Diff*, 1991, **6**, 2.
15. Page, T. F., Sawyer, G. R. and Discussion of microstructural characterization of, R. E. F. E.L., (reaction bonded) silicon carbides: authors' reply. *J. Mater. Sci.*, 1980, **15**, 1850–1856.
16. Ogbuji, L. U., Mitchell, T. W., Heuer, A. H. and Shinozaki, S., Discussion of microstructural characterization of REFEL (reaction bonded) silicon carbides. *J. Mat. Sci.*, 1979, **14**, 2267–2271.
17. Jepps, N. W. and Page, T. F., *Progress in Crystal Growth & Characterization*, 1983, **7**, 259–307.
18. Ness, J. N. and Page, T. F., Microstructural evolution in reaction bonded silicon carbide. *J. Mat. Sci.*, 1986, **21**, 1377–1397.